JOURNAL OF MATERIALS SCIENCE **37** (2002) 1019–1025

Fatigue behavior characterization of laser-welded cold rolled sheet metal (SPCEN)

KYONG Y. RHEE
School of Mechanical & Industrial System Engineering, Kyunghee University, 449-701 Korea

DAI-SOON KWAK
Department of Mechanical Engineering, Graduate School of Kyunghee University, 449-701 Korea

TAEK-YUL OH
School of Mechanical & Industrial System Engineering, Kyunghee University, 449-701 Korea

For the present work, the fatigue behavior of laser-welded cold-rolled sheet metal (SPCEN) was studied. Also, the thickness heterogeneity effect of weldment on the fatigue strength and crack growth behavior was studied. The sheet metals of same thickness (0.9 mm) were laser-welded (Case A), and the sheet metal of 0.9 mm thickness was laser-welded to the sheet metal of 2.0 mm thickness (Case B). For both cases, fatigue tests were conducted applying the load perpendicular or parallel to the welding line. Finite element analysis was performed to determine the form of stress intensity factor as a function of crack length for both cases. The results showed that the fatigue strength of Case A was 8.5% higher than that of Case B when the loading direction was parallel to the welding line. However, the fatigue strength of Case A was similar to that of Case B for the perpendicular fatigue loading to the welding line. At the same crack length, the stress intensity factor of Case A was greater than that of Case B. It was also found that for both cases, the crack propagation rate decreased noticeably in the front of weld bead but increased rapidly in the weld bead. The retardation of crack propagation was due to the increased hardness in the front of weld bead, and the increased crack propagation rate was due to the reduced fracture toughness in the weld bead.

1. Introduction

It is known that the laser welding is an effective welding method to improve the realiability and productivity of welded structure [1]. The advantage of laser welding over the conventional welding method is in the high welding speed, welding depth, and small deformation. Therefore, in recent years, the use of laser welding has increased significantly in the automobile industry [2, 3]. However, the current problem using the laser welding is the formability and structural stability of the welded structure. Accordingly, intensive research has been carried out to determine the optimal welding condition for the improvement of formability and structural stability [4–6]. For the research of structural stability, most of them have been related to the evaluation of fracture properties, and a small number of studies have been made to investigate the fatigue characteristics of laser-welded structure [7–9]. Particularly, the research result on the fatigue behavior of laser-welded structure of heterogeneous thickness is not available. However, it is often required to weld the structures of heterogeneous thickness in the automobile and shipbuilding industries. Thus, it is essential to study the fatigue characteristics of laser-welded structure of heterogeneous thickness in order that the laser welding can be used in a wide range as a welding method.

In the present work, the effect of thickness heterogeneity of weldment on the fatigue strength and crack growth behavior was studied. The effect of loading direction that can be parallel or perpendicular to the welding line on the fatigue behavior was also studied. Finite element analysis was performed to determine the form of stress intensity factor. The crack propagation rate was plotted as a function of crack length. Weld surface and fracture surface were examined by means of metallurgical microscope and scanning electron microscope (SEM) to determine the crack growth mechanism.

2. Experimental procedure

The material used in this study was SPCEN (KS D 3512) sheet metals of thickness, 0.9 mm and 2.0 mm. The chemical composition of SPCEN is indicated in Table I. The sheet metals of same thickness, 0.9 mm were laser-welded to each other. The sheet metal of thickness, 0.9 mm was also laser-welded to the sheet

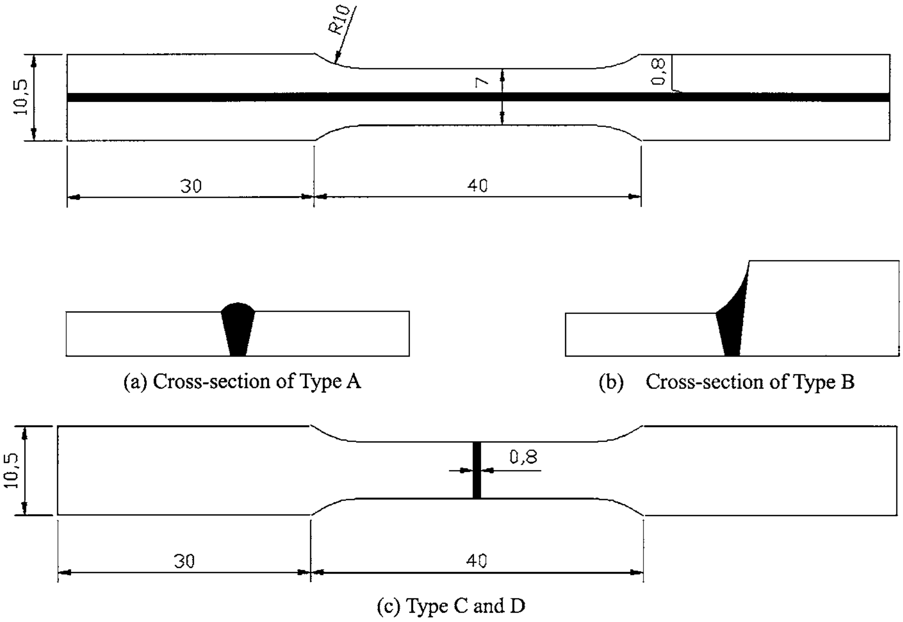

Figure 1 Schematic diagrams of for the fatigue strength test specimen (Type A, B, C and D).

TABLE I Chemical composition of SPCEN (wt%)

Material	C	Mn	Si	P	S
SPCEN	0.016	0.19	0.029	0.019	0.006

TABLE II Representation of test samples used for fatigue test

Type	Thickness (mm)	Loading vs. welding direction	Test
A	0.9 + 0.9	Parallel	Fatigue strength test
B	0.9 + 0.9	Perpendicular	Fatigue strength test
C	0.9 + 2.0	Parallel	(")
D	0.9 + 2.0	Perpendicular	(")
E	0.9 Base Metal	–	Crack propagation test
F	0.9 + 0.9	Parallel	Crack propagation test
G	0.9 + 2.0	Parallel	(")

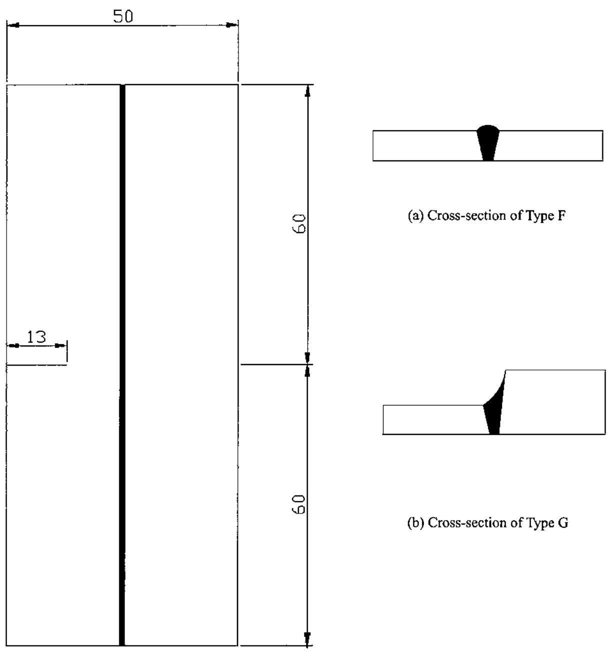

Figure 2 Schematic diagrams of specimen for the fatigue crack propagation test.

metal of thickness, 2.0 mm to investigate the effect of thickness heterogeneity on the fatigue behavior of laser-welded structure. Laser welding was made by using CO_2 laser under Helium (He) gas environment. The welding condition was as follows: welding power 4 kW and welding speed 5 m/min. Two kinds of test samples were made; one for fatigue strength test and the other for fatigue propagation test. Figs 1 and 2 show schematic diagrams of fatigue strength test sample and fatigue propagation test sample, respectively. For a fatigue propagation test, the pre-crack of 13 mm length was made at the edge by using a wire cutting machine. The samples used were summarized in Table II.

For the fatigue strength test, fatigue loading parallel or perpendicular to the weld line was applied to investigate the loading direction effect on the fatigue crack growth behavior. Fatigue tests were performed with an Instron machine (model: 8501) by applying a constant amplitude load of zero load ratio ($R = 0$). A sinusoidal loading shape and a loading frequency of 30 Hz were used. Fatigue strength was determined as the stress when the sample was fully fractured. For the fatigue propagation test, fatigue loading was parallel to the weld line while crack propagation was perpendicular to the weld line. Similar to the fatigue strength test, the fatigue propagation tests were performed with an Instron machine and the same conditions were applied except for a loading frequency that was applied at a frequency of 10 Hz. Fatigue tests were conducted at room temperature. Crack length was measured based on ASTM E647 by means of a travelling microscope ($100\times$) to an accuracy of 0.01 mm. Fracture surface was examined by using a scanning electron microscope. The hardness variation across the weld surface was also determined by means of the Micro Vickers hardness test.

Figure 3 Weld surface morphology of Type A specimen.

3. Results and discussion

3.1. Results of fatigue strength test

Fig. 3 shows the weld surface of "Type A" specimen taken by a metallurgical microscope. As shown in the figure, the weld bead is clearly visible in the middle and its width was about 0.8 mm. In order to determine the effect of laser welding on the microstructure of SPCEN, the microstructure of base metal, heat affected zone (HAZ), and weld bead was examined.

Fig. 4 shows the microstructures of base metal (a), HAZ (b), and weld bead (c) taken by a metallurgical microscope. It can be seen that the microstructure of base metal is different from that of weld bead. The typical grain shape and its boundary of SPCEN are shown in the base metal while the grain shape and its boundary are collapsed in the weld bead. Particularly, it can be seen that the boundary line between the base metal and the weld bead was clear with a narrow HAZ. This indicates that the HAZ was minimized, which represents the advantage using the laser welding. The reason why HAZ is minimized when the laser welding is applied is that most of the welding energy is concentrated to the local area.

The hardness measurement of base metal, HAZ, and the bead was made from the Micro Vickers hardness test at regular intervals of 0.25 mm along the weld surface. Fig. 5 shows the variation of hardness along the base metal, HAZ, and the weld bead. As shown in the figure, the hardness did not change in the base metal and HAZ. However, it increased significantly at the weld bead. Specifically, the hardness of base metal was 85 HV and that of weld bead was 192 HV, which was 2.3 times higher than the hardness of base metal. The abrupt increase of hardness in the weld bead was due to the narrow HAZ as described earlier.

The effect of loading direction on the fatigue strength was determined. Fig. 6 shows a comparison of fatigue strength of "Type A" and "Type B" cases (welded structure of same thickness). As shown in the figure, the fatigue strength of "Type B" specimen was lower than that of "Type A" specimen. Fig. 7 shows a comparison of fatigue strength of "Type C" and "Type D" cases (welded structure of heterogeneous thickness). Similar to the case of same thickness, the fatigue strength of "Type D" was lower than that of "Type C". That is, the specimen loaded parallel to the weld line resulted in higher fatigue strength than the specimen loaded

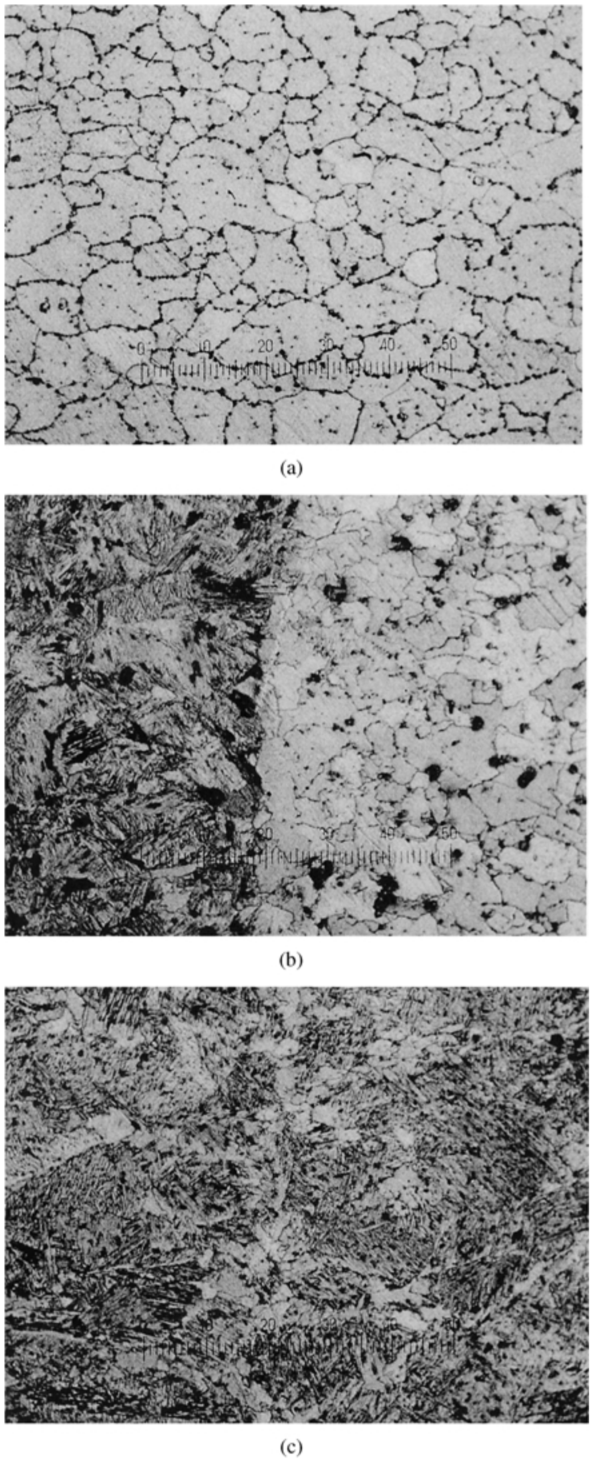

Figure 4 Microstructures of base metal (a), HAZ (b) and weld bead (c).

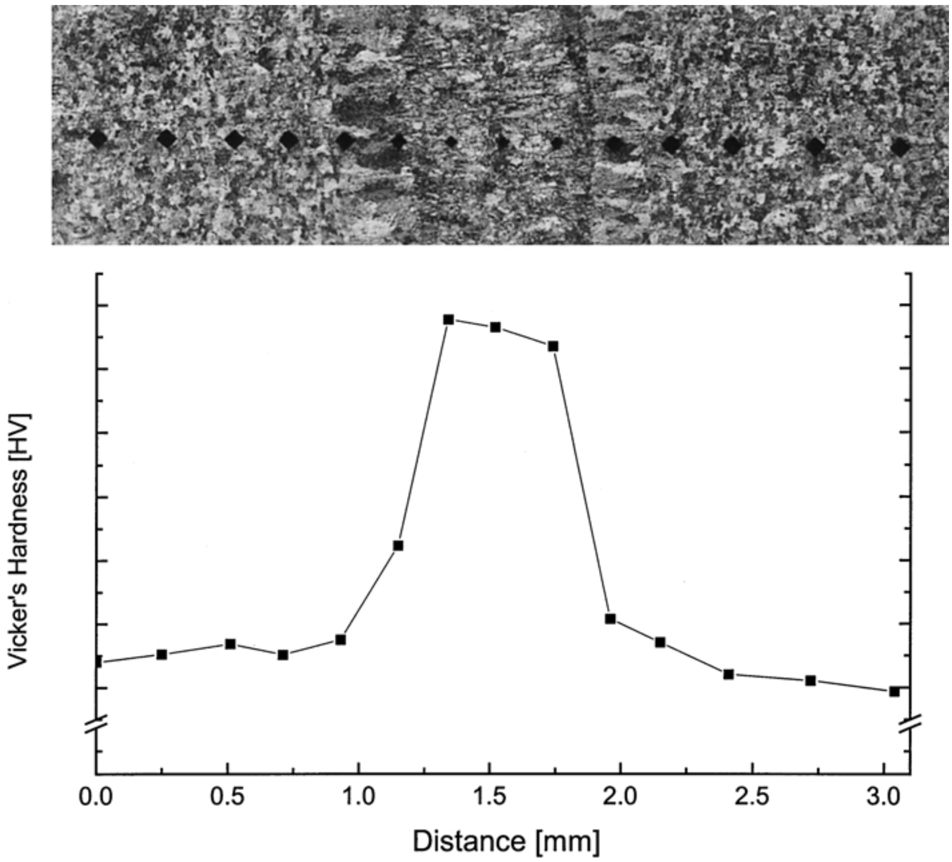

Figure 5 Variation of hardness along the base metal, HAZ and the weld bead.

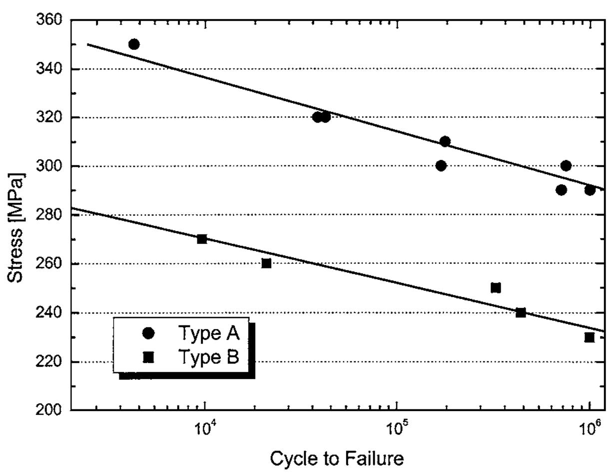

Figure 6 Effect of loading direction on fatigue strength for the welded structure of same thickness.

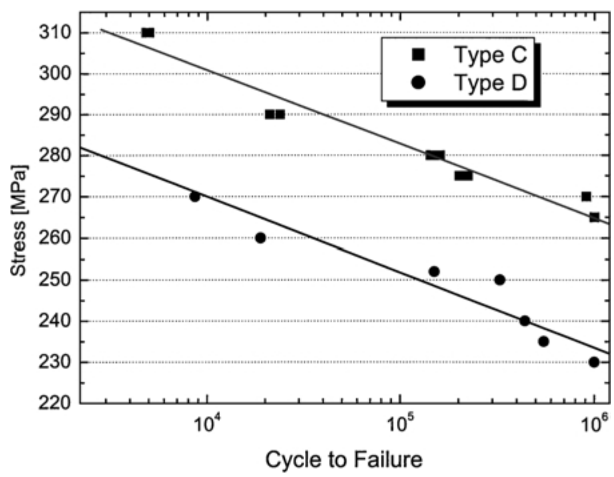

Figure 7 Effect of loading direction on fatigue strength for the welded structure of heterogeneous thickness.

perpendicular to the weld line. The phenomenon can be explained by considering where the crack was initiated and final fracture occurred. For the specimens loaded perpendicular to the weld line ("Type B" and "Type D"), crack was initiated in the base metal and the final fracture also occurred in the base metal. For the specimens loaded parallel to the weld line ("Type A" and "Type C"), however, crack was initiated in the weld bead and the final fracture occurred in the base metal. The crack initiation of "Type B" and "Type D" cases in the base metal was attributed to the higher fatigue resistance of weld bead than the base metal. The crack initiation of "Type A" and "Type C" cases in the weld bead was attributed to the strain constraint caused by strength discontinuity that was due to the hardness discrepancy between the weld bead and the base metal.

In order to determine the effect of thickness heterogeneity on the fatigue strength, the fatigue strength of "Type A" case was compared with that of "Type C" case. Fig. 8 shows the comparison of fatigue strength results. As shown in the figure, the fatigue strength of "Type C" was about 8.5% lower than that of "Type A". Specifically, the fatigue strength of "Type A" was a 290 MPa and that of "Type C" was a 265 Mpa. The lower strength of "Type C" was attributed to the notch effect. That is, the discontinuous face due to different

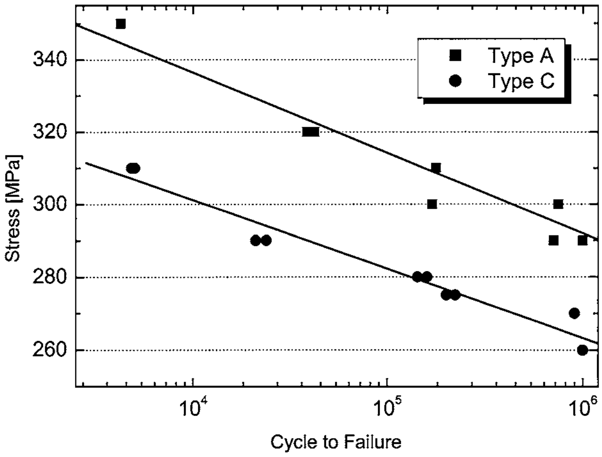

Figure 8 Effect of heterogeneity on the fatigue strength.

thickness worked as a notch at the interface and induced a higher stress concentration, which resulted in the decreased fatigue strength.

Fig. 9 shows the photographs of fractured specimen of "Type A" (a) and "Type C" (b). For a specimen of "Type A", crack was initiated from the flat area in the middle that was a weld bead. Then, the crack propagated symmetrically to both sides of the base metal. For a specimen of "Type C", crack was initiated in the weld bead. However, the crack did not propagate symmetrically but grew more in the thicker base metal. The unsymmetrical crack propagation of "Type C" was attributed to the large strain constraint effect as described earlier.

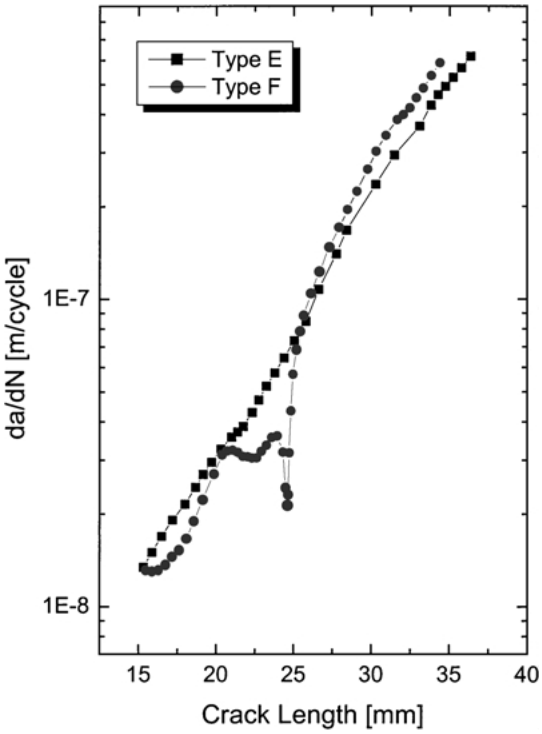

Figure 10 Fatigue crack propagation behavior of welded structure of the same thickness.

3.2. Results of fatigue crack propagation test

In order to determine the laser-weld effect on the crack propagation behavior, the crack propagation of welded structure was compared with that of base metal. Fig. 10

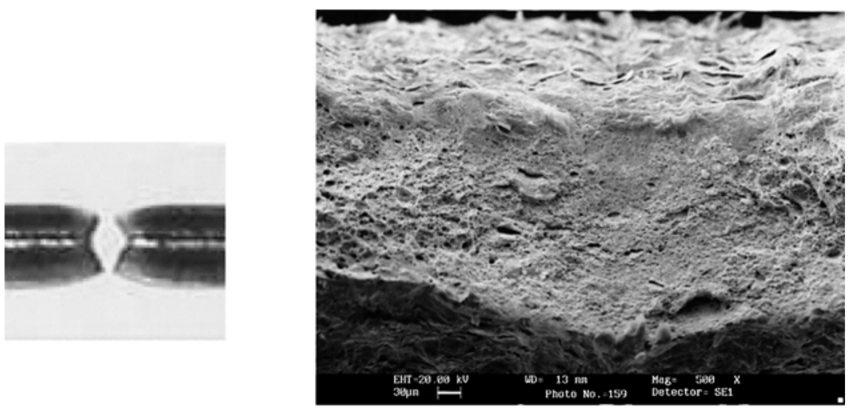

(a)

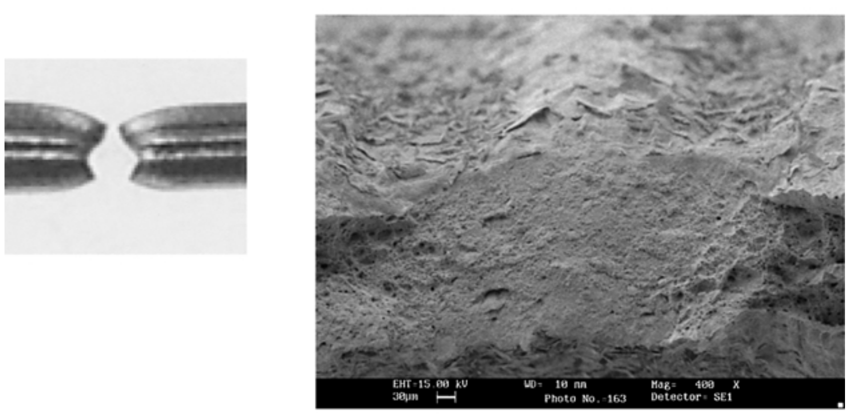

(b)

Figure 9 Photographs of fractured specimens: Type A (a) and Type D (b).

shows a comparison of crack propagation rate versus crack length for a "Type E" (base metal, 0.9 mm) and a "Type F" (welded structure of same thickness, 0.9 mm + 0.9 mm). The crack propagation rate was determined from the seven point method [10]. As shown in the figure, the specimen of "Type E" exhibited a typical crack propagation behavior. The specimen of "Type F" also exhibited a normal crack propagation behavior before the crack reached the weld bead. However, a crack retardation occurred when the crack reached the weld bead. Then, the crack propagated fast along the weld bead and resumed a normal crack propagation behavior again once it passed through the weld bead. It seems that the crack retardation was attributed to the strength discontinuity and residual stress at the weld bead. It can be seen in the figure that the crack propagation of "Type F" was similar to that of "Type E" before and after the weld bead. This indicates that the effect of HAZ and weld bead on the fatigue behavior is not significant in the laser welding.

The crack propagation rate of "Type F" specimen was compared with that of "Type G" specimen (welded structure of heterogeneous thickness, 0.9 mm + 2.0 mm) to determine the effect of thickness heterogeneity. Fatigue load was adjusted for the specimen of "Type G" in order to apply the same stress given to the "Type F" specimen to the thin plate and the thick plate. Fig. 11 shows the comparison of crack propagation rate for both specimens. It can be seen in the figure that the crack retardation also occurred at the weld bead for the specimen of "Type G". It can be also seen that the crack propagation rate of "Type G" specimen was the same as that of "Type F" specimen until the crack propagated 2 mm where the initial crack length was a 13 mm. After the crack propagated 2 mm, the crack propagation rate of "Type G" specimen was lower than that of "Type F" specimen. The reason for the low crack propagation is that the specimen of "Type G" has a discontinuous thickness. The discontinuous thickness worked as a notch and led to a smaller load application to the thin plate.

Finite element analysis was performed for "Type F" and "Type G" specimens to determine the stress intensity factor as a function of crack length because the crack propagation rate can be related to stress intensity factor. For the present study, the stress intensity factor was determined from CTOD method by neglecting the residual stress. Fig. 12 shows the finite element meshes at the crack tip used for "Type F" and "Type G" specimens.

Fig. 13 shows the variation of stress intensity factor with crack increase for both specimens. As can be

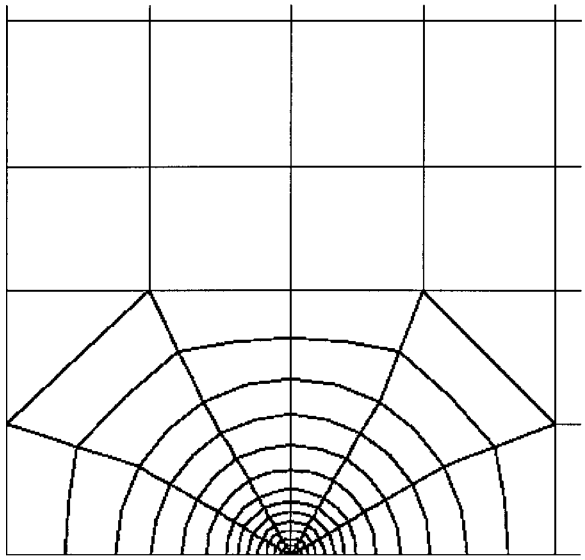

Figure 12 Finite element meshes at the crack tip.

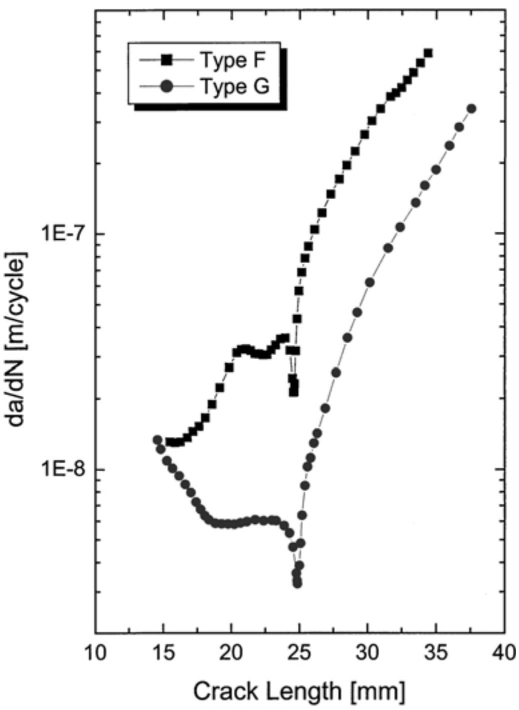

Figure 11 Fatigue crack propagation behavior of welded structure of heterogeneous thickness.

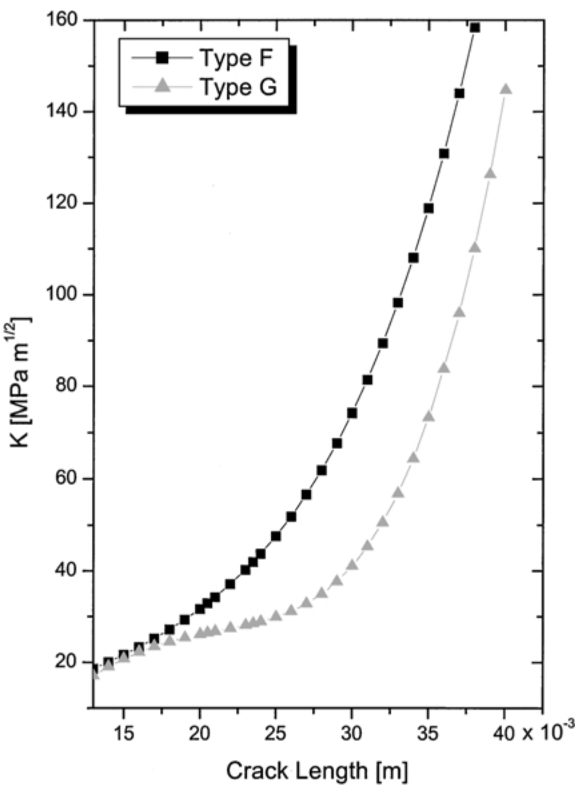

Figure 13 Variation of stress intensity factor as a function of crack length for Type F and Type G.

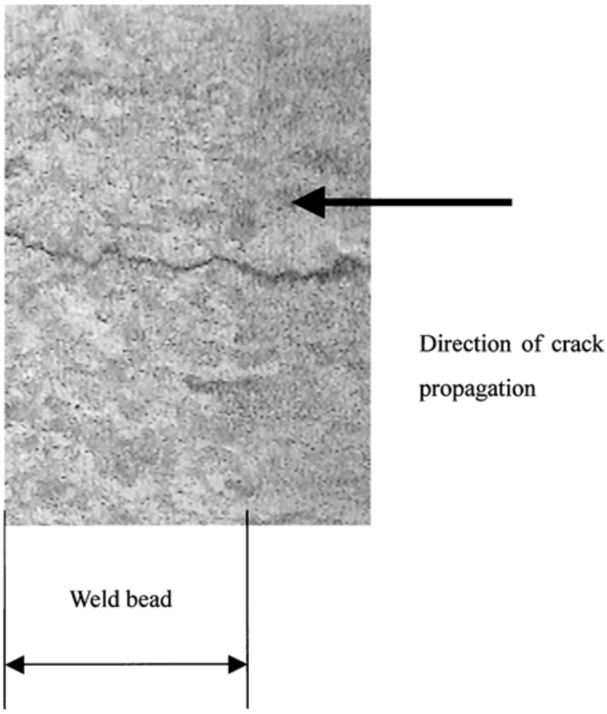

Figure 14 Photograph of cracked weld-surface of Type F.

seen in the figure, the stress intensity factors of both specimens are similar when the crack length is short. Then, as the crack propagates more, the stress intensity factor of "Type G" specimen becomes smaller than that of "Type F" specimen. This agrees well with the experimental results that the crack propagation rate of "Type G" specimen was lower than that of "Type F" specimen.

The cracked weld-surface was examined by means of optical microscope to investigate the crack shape around the weld bead. Fig. 14 shows the cracked weld-surface of "Type F" specimen. As can be seen in the figure, the crack shape in the weld bead is different from that before the weld bead. The width of crack was wide before the crack reached the weld bead. However, the crack became narrow in the weld bead. The narrow crack was attributed to the increased hardness in the weld bead. Thus, it can be explained that the crack retardation in the front of weld bead was caused by wide crack, and the fast crack propagation in the weld bead was caused by the decreased fracture toughness due to the increased hardness.

4. Conclusion

In this study, the thickness heterogeneity effect on the fatigue strength and crack growth behavior in the laser welding was investigated. The loading direction effect on the fatigue behavior was also investigated. Followings are the conclusions obtained from the present study.

1. The specimen loaded parallel to the weld line resulted in higher fatigue strength than the specimen loaded perpendicular to the weld line.
2. Fatigue strength was affected by the thickness heterogeneity of weldment. The fatigue strength of heterogeneous thickness case was about 8.5% lower than that of same thickness case. The lower strength of heterogeneous thickness case was attributed to the discontinuous face that worked as a notch.
3. The crack propagation rate of heterogeneous thickness case was lower than that of same thickness case. For both cases, the crack retardation occurred in the front of weld bead and the fast crack propagation occurred at the weld bead. The fast crack propagation was attributed to the decreased fracture toughness caused by the increased hardness.

Acknowledgement

This work was supported by Ministry of Science and Technology as a part of the Nuclear R&D Program.

References

1. A. J. SELIGE and W. PRANGE, Production and usage of laser-beam-welded sheet metal, SAE 870413.
2. W. PRANGE, C. SCHNEIDER and A. J. SELIGE, Application of laser-beam-welded sheet metal, SAE 890853.
3. L. HANICKE and O. STRANDBERG, Roof laser welding in series production, SAE 93002.
4. M. EISENMENGER, K. K. BHATT and M. F. SHI, Influence of laser welding parameters on formability and robustness of blank manufacturing: an application to a body side frame, SAE 950922.
5. R. P. MARTUKANITZ, B. ALTSHULLER, F. G. ARMAO and E. R. PICKERING, Properties and characteristics of laser beam welds of automotive Al alloys, SAE 960168.
6. H. POTENTE and F. BECKER, Weld strength behavior of laser butt welds, ANTEC (1999).
7. JIUN-REN HWANG, JI-LIANG DOONG and CHEE-CHANG CHEN, *Materials Transactions, JIM* **37**(8) (1996) 1443.
8. B. Y. WANG, M. F. SHI, H. SADRNIA and F. LIN, Structural performance of tailor welded sheet steels, SAE 950376.
9. J. ONORO and C. RANNINGER, *Journal of Materials Processing Technology* **68** (1997) 68.
10. Standard test method for measurement of fatigue crack growth rates, ASTM Standards E 647 (1993).

Received 11 October 2000
and accepted 13 August 2001